Electronic Properties of Hydrogen Storage Materials with Photon-in/Photon-out Soft-X-Ray Spectroscopy

Jinghua Guo

Advanced Light Source, Lawrence Berkeley National Laboratory, Berkeley, CA 94720

Abstract

The applications of resonant soft X-ray emission spectroscopy on a variety of carbon systems have yielded characteristic fingerprints. With high-resolution monochromatized synchrotron radiation excitation, resonant inelastic X-ray scattering has emerged as a new source of information about electronic structure and excitation dynamics. Photon-in/photon-out soft-x-ray spectroscopy is used to study the electronic properties of fundamental materials, nanostructure, and complex hydrides and will offer potential in-depth understanding of chemisorption and/or physisorption mechanisms of hydrogen adsorption/desorption capacity and kinetics.

The primary challenge of using more hydrogen in our energy systems is the cost of producing, storing, and transporting the hydrogen. Of all these, hydrogen storage is the most challenging task for developing the hydrogen economy. Chemical-based solid-state hydrogen storage methods use materials that retain hydrogen, which can subsequently be released by heating or via a chemical reaction. These systems have the potential for greater onboard fuel capacity than compressed gas or liquid hydrogen systems. However, they are still at an early stage of development.

The basic requirements for effective hydrogen storage include high storage capacity with high gravimetric and volumetric densities, fast kinetics to enable quick uptake and release, a long cycle lifetime for hydrogen adsorption/desotrption, and effective heat transfer [1,2]. The development of hydrogen-fueled vehicles and portable electronics will require new materials that can store large amounts of hydrogen at ambient temperature and relatively low pressures with small volume, low weight, and fast kinetics for recharging. A design target for automobile fueling (FreedomCAR project) has been set by the U.S. Department of Energy at 6 wt% and 9 wt% hydrogen storage capacity in 2010 and 2015, respectively.

Hydrides offer the advantage of high storage densities per unit volume that are 60% higher than those of liquid hydrogen at 20K, and approximately seven times above that of compressed gas at a pressure of 200 bar [3]. There are two basic hydride families of intermetallic compounds: metal or interstitial hydrides and complex hydrides. Both metal and complex hydrides suffer from high thermal stability (hydrogen desorption temperature > 250°C) and/or slow kinetics, which prevent these materials from practical applications [4,5].

Our concept is to exploit the electronic properties of hydrogen storage materials to gain insight into hydrogen adsorption in metal and complex hydrides, doping- and defect-induced hydrogen adsorption/desorption, combined chemisorption and physisorption mechanism for hydrogen storage using metastable nanoporous hydride materials and carbon nanostructures, and new classes of hydrogen storage materials, for example, carbon nanostructured materials and metal organic framework.

Based on photon-in/photon-out soft-x-ray spectroscopy, we aim for in-depth

understanding of the mechanisms to increase the hydrogen-storage capacity and to improve the hydrogen-storage kinetics. Soft-x-ray absorption probes the local *unoccupied* electronic structure; soft-x-ray emission probes the *occupied* electronic structure; and the addition of resonant inelastic soft-x-ray scattering (Raman spectroscopy with soft x-rays) opens a new field of study by disclosing many new possibilities for photon-in/photon-out soft-x-ray spectroscopy [6,7].

Hydrogen storage reactions require a control of kinetics and interface under well-defined temperature and pressure, which is as important as designing new materials. Such an effort requires the continual development of new experimental techniques and methodologies. We have demonstrated the usefulness of soft-x-ray spectroscopic studies of liquids, gases, and solid samples in a gaseous environment.

We have used the experimental equipment at beamline 7.0 at ALS, which is equipped with a SGM monochromator with a resolving power of 4000 in the energy range of 80-1000 eV appropriate for studying the fundamental electronic properties and chemisorption and/or physisorption mechanisms of hydrogen storage materials. Soft x-rays require a vacuum environment in the beamline and fluorescence spectrometer. Thus, the gaseous and liquid-phase samples will be maintained in cells inside the vacuum chamber with windows to allow the penetration of soft x-rays. In the soft-x-ray regime, the attenuation length of photons is typically hundreds of nanometers in solid matter. The penetration depth offers experimental opportunities not present in electron-based spectroscopy. This offers the possibility to study hydrides confined in a closed volume, such as a solid-state hydride sample exposed to hydrogen gas in the sample cell. One of major challenge for the hydrogen cell is find a suitable thin window to be transparent for soft x-rays and strong to maintain the pressure for hydrogen reactions. Currently we use 100-nm-thick silicon-nitride membrane for liquid and gas cells.

Using x-ray absorption spectroscopy (XAS) and selectively excited x-ray emission spectroscopy (XES) to probe unoccupied and occupied electronic states, one can establish a firm interpretation for the unusual thermodynamic properties of molecular liquids. Furthermore, one can elucidate finer details of their structural properties. XAS and XES spectra reflect the local electronic structure of the various conformations. XES spectra,

emanating from the radiative decay, subsequent to core excitation, can be useful in assigning structures in XAS spectra [8-11].

Chemical sensitivity is obtained when the resolution of the detected emission lines is high enough to resolve fine structure. The line shapes are determined by the valence electron distribution and the transitions are governed by dipole selection rules. For solids, essentially a partial DOS mapping is obtained. This is exemplified by the carbon K-edge absorption and emission spectra of the carbon solids.

The difference in structural arrangement of these allotropic forms of carbon gives rise to the wide differences in their physical properties. Carbon has an atomic number of 6 and has the $1s^2 2s^2 2p^2$ configuration in its electronic ground states. The sp-orbital, and the sp^3-hybrid orbital indicate rotational symmetry. Bonds of this kind are called σ-bonds. The electrons involved in such bonds are called σ-electrons. With double bonds in sp^2-hybdrid orbitals, so-called π-orbitals occur with corresponding π-electrons. Such orbitals are not symmetrical with regard to their bonding orientation.

The normal carbon K-edge x-ray and absorption and emission spectra of diamond, graphitic carbon, C_{70}, C_{60}, and benzene are presented in Figure 1, where large differences in spectral profile are observed. The spectra of diamond and graphitic carbon show a wide band with some shoulder structures, where the energy positions of the peak maximum and band shapes are largely different. In some studies related to vapor deposition, the x-ray emission spectral profile has been used as a means to identify certain chemical states [12,13]. In contrast, the spectra of benzene, C_{60}, and C_{70} exhibit clearly resolved emission peaks, indicating strong molecular character in their solid phase. The marked resolved emission features in benzene can find their counterpart in the emission spectra of C_{60} and C_{70}, and all the fine structures are washed out in diamond and graphite.

The x-ray absorption spectral shape of carbon nanotubes is similar to that of HOPG, which is different from that of C_{60}. The π* shows a shift towards low photon energy in the x-ray absorption of C-nanotubes. C_{60} gives more resolved absorption features, which indicate a strong molecular character of C_{60}. Non-resonant carbon *K*-edge emission spectra of carbon nanotubes and C_{60} show a similar shape, but resonantly excited K-edge

emission spectra reveal large differences in the electronic structure of these two systems. The x-ray absorption spectrum of diamond shows no π^* contribution, and the absorption feature at 288.8 eV is the diamond exciton.

The interaction of titanium and C_{60} in co-evaporated Ti intercalated C_{60} has been investigated by using XAS, XES, and detuning excited XES [14,15]. The RIXS spectra of Ti-C_{60} are different to that of pure C_{60} (seen in Figure 2). On excitation below π^* resonance the spectra show a remarkable excitation energy dependence, which has been discussed in detail for pure C_{60} [16]. The RIXS spectra of the Ti-C_{60} sample have, in addition to a C_{60}-like dispersing peak, a feature at constant emission energy, around 277-279 eV. The dispersion properties in the RIXS spectra of the Ti-C_{60} sample can thus be used to assign the states that are reached at the various excitation energies. The dispersing C_{60}-like feature is associated with excitations to the C_{60} π^*-like strong absorption resonance, whereas the non-dispersive feature is due to excitations to the first metal-like states just above the Fermi level.

Note that these states, which can hardly be observed in direct absorption, give an essential contribution to the RIXS spectra, and thus, information about the carbon-titanium bonding. By examining the threshold-excited RIXS spectra of the Ti-C_{60} sample, the symmetry of the first unoccupied orbitals can now be readily determined. The C_{60}-like dispersing feature is indicative of t_{1u}-like symmetry. The C_{60} π^* orbital largely retains its character as it hybridizes with the metal orbitals. On the other hand, it is immediately obvious that the non-dispersing feature at 277-279 eV emission energy cannot be due to excitations of the same symmetry. Instead this part of the spectrum can be explained by assuming that the first unoccupied states are of h_u-like symmetry.

Hydrogen strongly affects the electronic and structural properties of many materials. In terms of electronic structure, the proton acts as an attractive potential to the host metal electrons; electronic bands are lowered in energy and form low-lying bands by hybridization with the hydrogen band. The change of electronic structure and energy bandgap as a result of hydrogen adsorption/desorption was demonstrated in the study of metal hydrides [17,18]. For example, the photographs in Figure 3(top) show the behavior of a 500-nm-thick yttrium film covered with a 20-nm palladium layer [19]. The yttrium

film before hydrogenation (top left) is metallic and all the photons in the visible range are reflected. The mirror image of the knight is clearly visible. The film after hydrogen uptake (top right) is in the trihydride phase and has become transparent shown by the visibility of the chess-board pattern. The hydrogenation can be understood by means of soft-x-ray spectroscopy. Figure 3(bottom) shows the Y-$M_{4,5}$ x-ray fluorescence and absorption spectra from Y, YH_2, and YH_3. We can see the metallic character of yttrium, i.e., the finite density of states at the intersection of the soft-x-ray emission and absorption spectra (Fermi level). For YH_2, hybridization states appear at binding energy of 7 eV and a finite density of states remains at the Fermi level. For YH_3, a 2.5-eV band gap has opened up, which indicated the MIT from yttrium metal to yttrium tri-hydride. In one of the experiments performed earlier, a pressure of 100-torr H_2 was sealed in a Si_3N_4-windowed cell [17].

In summary, we have demonstrated utilization of soft-x-ray spectroscopy as a unique method for studying the fundamental electronic properties and chemisorption and/or physisorption mechanisms of hydrogen storage materials. Most of the proposed experiments are very photon hungry and thus require the use of 3rd generation soft-x-ray synchrotron radiation facility such as the ALS. Considerable sample freedom is offered, and adsorbates, thin films, solids, and buried structures can be studied with and without the presence of a hydrogen atmosphere.

References

1. Argonne National Laboratory, Basic research needs for the hydrogen economy, Report of the Basic Sciences Workshop on Hydrogen Production, Storage, and Use (Chaired by Mildred D. Dresselhaus), May 13-15, 2003. http://www.sc.doe.gov/bes/hydrogen.pdf;

2. L. Schlapbach and A. Zuttle, Hydrogen-storage materials for mobile applications, Nature, vol. 414, pp.353, 2001

3. A. M. Seayad, D. M. Antonelli, Recent advances in hydrogen storage in metal-containing inorganic nanostructures and related materials, Advanced Materials, vol. 16, pp. 765-777, 2004

4. J. J. Reilly, R. H. Wiswall, Reaction of hydrogen with alloys of magnesium and copper, Inorganic Chemistry, vol. 6, pp. 2220-2223, 1967

5. K. J. Gross, G. J. Thomas, C. M. Jensen, Catalyzed alanates for hydrogen storage, Journal of Alloys and Compounds, vol. 330, pp. 683-690, 2002

6. S. M. Butorin, J.-H. Guo, M. Magnuson, P. Kuiper, J. Nordgren, Low-energy *dd* excitations in MnO studied by resonant X-ray fluorescence spectroscopy, Phys. Rev. B vol. 54, pp. 4405, 1996

7. P. Kuiper, J.-H. Guo, C. Såthe, L.-C. Duda, J. Nordgren, J. J. M. Pothuizen, F. M. F. de Groot, G. A. Sawatzky, Resonant X-ray Raman spectra of Cu *dd* excitations in $Sr_2CuO_2Cl_2$, Phys. Rev. Lett. vol. 80, pp. 5204, 1998

8. K. Gunnelin, P. Glans, P. Skytt, J.-H. Guo, J. Nordgren, and H. Ågren, Assigning x-ray absorption spectra by means of soft-x-ray emission spectroscopy, Phys. Rev. A vol. 57, pp. 864-872, 1998

9. N. Hellgren, J.-H. Guo, C. Såthe, A. Agui, J. Nordgren, Y. Luo, H. Ågren , and J.-E. Sundgren, Nitrogen Bonding Structure in Carbon Nitride Thin Films Studied by Soft X-ray Spectroscopy, Appl. Phys. Lett. vol. 79, pp. 4348-4350, 2001

10. J.-H. Guo, Y. Luo, A. Augustsson, J.-E. Rubensson, C. Såthe, H. Ågren, H. Siegbahn, and J. Nordgren, X-ray Emission Spectroscopy of Hydrogen Bonding and Electronic Structure of Liquid Water, Phys. Rev. Lett., vol. 89, pp. 137402, 2002

11. J.-H. Guo, Y. Luo, A. Augustsson, S. Kashtanov, J.-E. Rubensson, D. K. Shuh, H. Agren, and J. Nordgren, The molecular structure of alcohol-water mixtures, Phys. Rev. Lett., vol. 91, pp. 157401, 2003

12. J.-H. Guo, J. Nordgren, Resonant C $K\alpha$ X-ray emission of some carbon allotropes and organic compounds, J. Electr. Spectr. vol. 110-111, 105-134, 2000

13. J.-H. Guo, Synchrotron radiation, soft-X-ray spectroscopy and nanomaterials, Int. J. Nanotechnology vol. 1-2, pp. 93-225, 2004

14. L. Qian, M. Nyberg, Y. Luo, J.-E. Rubensson, A. V. Talyzine, C. Såthe, D. Ding, J.-H. Guo, H. Högberg, T. Käämbre, U. Jansson, and J. Nordgren, Bonding mechanism in the transition-metal fullerides studied by symmetry-selective resonant x-ray inelastic scattering, Phys. Rev. B vol. 63, pp. 84518, 2001

15. Mats Nyberg, Yi Luo, L. Qian, J.-E. Rubensson, C. Såthe, D. Ding, J.-H. Guo, T. Käämbre, and J. Nordgren, Bond formation in titanium fulleride compounds studied through x-ray emission spectroscopy, Phys. Rev. B vol. 63, pp. 115117, 2001

16. J.-H. Guo, P. Glans, P. Skytt, N. Wassdahl, J. Nordgren, Y. Luo, H. Ågren, Y. Ma, T. Warwick, P. Heimenn, E. Rotenberger, and J. Denlinger, Resonant X-ray Fluorescence from C_{60}, Phys. Rev. B vol. 52, pp. 10681, 1995

17. L.-C. Duda, P. Isberg, P. H. Andersson, P. Skytt, B. Hjörvarsson, J.-H. Guo et al., Hydrogen-Induced Changes of the Electronic States in Ultrathin Single-Crystal Vanadium Layers, Phys. Rev. B, vol. 55, pp. 12914, 1997

18. B. Hjörvarsson, J.-H. Guo et al., Probing the local electronic structure in the H induced metal-insulator transition of Y, J. Phys.: Cond. Mat., vol. 11, pp. L119, 1999

19. J. N. Huiberts et al., Yttrium and lanthanum hydride films with switchable optical properties, Nature, vol. 380, pp. 231-234, 1996
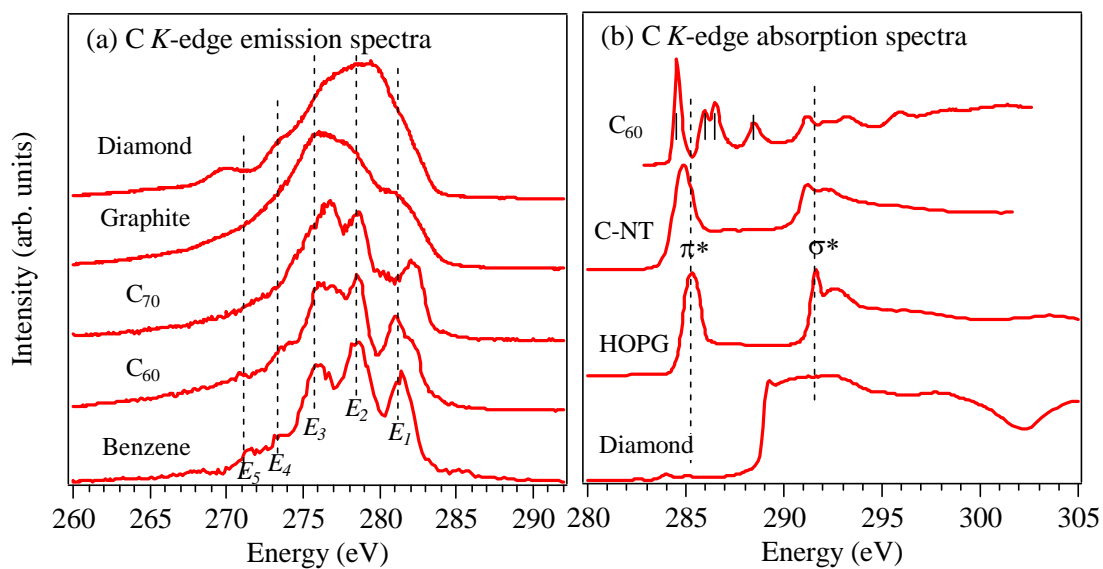
Figure 1

Figure 1. (a) Normal carbon K-edge emission spectra of diamond, amorphous carbon (graphitic), C_{70}, C_{60}, and benzene; (b) X-ray absorption spectra of C_{60}, carbon nanotubes, HOPG, and diamond.

Figure 2

QuickTime™ and a
TIFF (LZW) decompressor
are needed to see this picture.

Figure 2. Experimental and theoretical RIXS spectra of C_{60} (lower left) and the Ti-C_{60} (lower right) are recorded at selected excitations near the π resonance (284.5 eV) and below. XAS absorption spectra are at top with arrows indicating the excitations.

Figure 3

Object   Yttrium mirror   Yttrium hydride

X-ray emission   X-ray absorption

VB   CB

YH₃

YH₂

Y

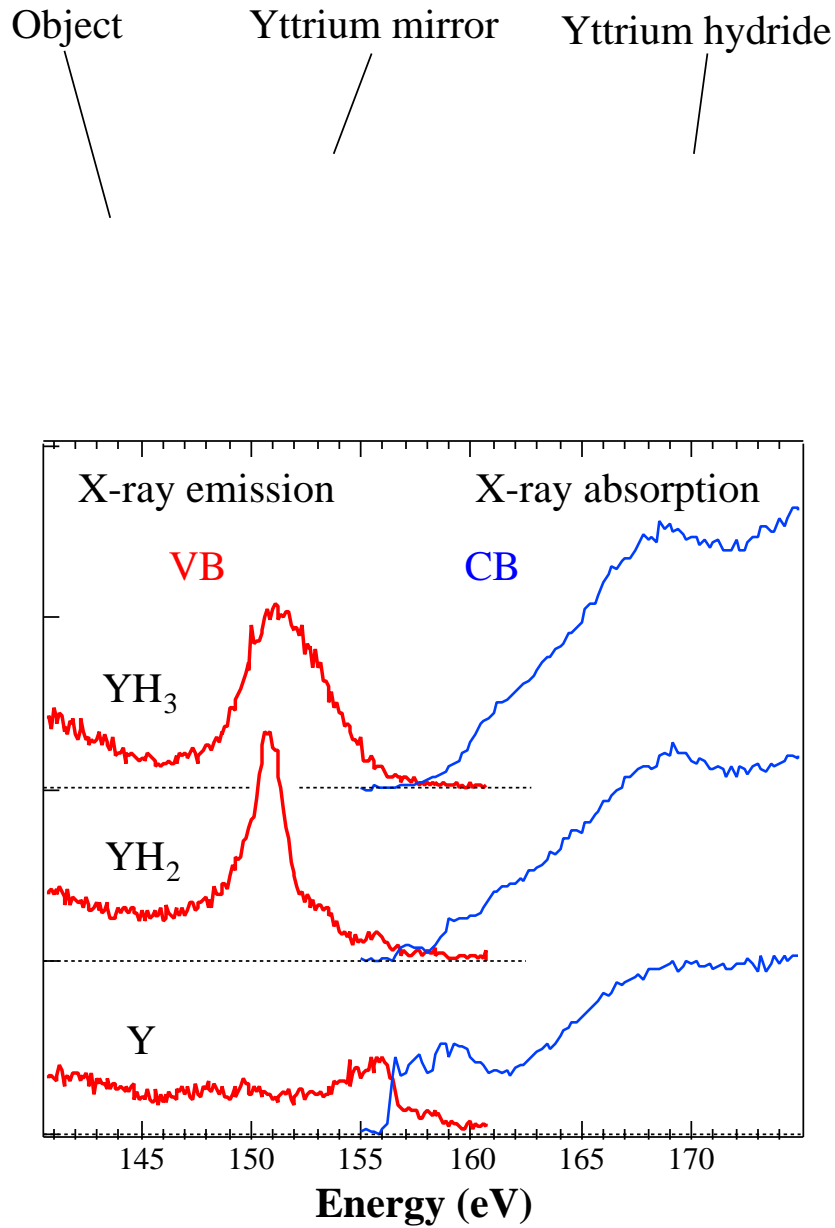145   150   155   160   165   170

Energy (eV)

Figure 3. The yttrium film is mirror before hydrogenation (top left) and becomes transparent after loaded with hydrogen (top right) [Huiberts et al. Nature 1996]; Soft-x-ray spectra map the occupied and unoccupied electronic structure and show metal and insulator transitions of Y hydrides (bottom).